NJC

Accepted Manuscript

ROYAL SOCIETY OF CHEMISTRY

www.rsc.org/njc

NJC

PAPER

New Journal of Chemistry Accepted Manuscript

Poly(glycidyl methacrylate) Coated Dual Mode Upconverting Nanoparticles For Neuronal Cell Imaging

Nicole M. Smith,[a,b*†] Diwei Ho,[b†] Alaa Munshi,[b] Michael J. House,[c] Sarah A. Dunlop,[a] Melinda Fitzgerald,[a] and K. Swaminathan Iyer[b]

Lanthanide-doped upconversion nanoparticles are promising dual mode near-infrared (NIR) and magnetic resonance imaging (MRI) bioimaging agents. In this communication we report the utility of $NaGdF_4$:Yb,Er nanoparticles with a functional poly(glycidyl methacrylate) (PGMA) coating, as a biocompatible multimodal formulation for neuronal cell imaging.

Introduction

High resolution fluorescence imaging has been a tool of enormous importance, increasing understanding of localization of proteins, the nature of cellular processes, and gene expression in live cells.[1] Conventional fluorescence imaging probes rely on ultraviolet (UV) light as the excitation source. However, they suffer drawbacks from auto-fluorescence and scattering by various biological molecules. Importantly, prolonged exposure of the biological samples to UV radiation can cause sample photodamage and mutation.[2] This can be overcome using near-infrared (NIR) fluorescence imaging which permits high signal-to-noise ratio and deep tissue penetration.[2,3] However, commonly used NIR chromophores suffer from poor photostability and biocompatability.[2,3] Furthermore, these fluorescent probes have broad emission spectra unsuitable for multiplex biolabeling.[2] These drawbacks have prompted research in the development and application of lanthanide-doped upconversion (UC) nanoparticles that rely on their unusual non-linear optical properties to convert two or more low-energy pump photons to a higher-energy output photon.[4-13] Consequently, these UC nanoparticles exhibit anti-Stokes emission upon low levels of irradiation in the near-infrared (NIR) spectral region, where biological molecules are optically transparent. Importantly, UC nanoparticles show sharp emission bandwidth, long lifetime, tunable emission and very high photostability.[11-12] Additionally, the unusual magnetic and optical properties associated with f-electrons of lanthanide elements make them highly suitable for the development of multimodal platforms, which combine both magnetic and upconversion fluorescent properties in a single nanoparticle construct.[14] These features can be integrated within single particles upon proper choices of particle matrix and dopants.[15-22]

Application of nanoparticles in neuroscience has garnered much attention in the recent past. Nanotechnologies have enabled advanced imaging, development of nanoscale scaffolds for neural regeneration, neuroprotection, and delivery of drugs across the blood–brain barrier.[23] In this current communication we report the fabrication of poly(glycidyl methacrylate) (PGMA) coated magnetic/upconversion fluorescent $NaGdF_4$:Yb,Er nanoparticles and demonstrate their biocompatibility as multimodal agents using rat pheochromocytoma neural progenitor (PC-12) cell lines. The developed formulation will enable tracking of the nanoparticles using a combination of imaging modalities; magnetic resonance imaging (MRI) due to the presence of Gd in the nanoparticles, and NIR fluorescence microscopy by the virtue of the upconversion capability of $NaGdF_4$:Yb,Er. Our approach will combine the radiation-free, whole-body, deep tissue imaging ability of MRI with the sensitivity of fluorescence detection. Importantly, the PGMA polymer contains epoxide groups which enable anchoring of a range of functional moieties by means of a simple epoxide ring-opening reaction to tailor the surface properties. This ease of tunability of surface is an important feature which enables tethering a range of biological moieties like antibodies,

a. *Experimental and Regenerative Neurosciences, School of Animal Biology, The University of Western Australia, 35 Stirling Hwy, Crawley WA 6009, Australia. nicole.smith@uwa.edu.au*

b. *School of Chemistry and Biochemistry, The University of Western Australia, 35 Stirling Hwy, Crawley WA 6009, Australia.*

c. *School of Physics, The University of Western Australia, 35 Stirling Hwy, Crawley WA 6009, Australia.*

d. † *The authors contributed equally to the work.*

peptides and proteins to enable medical translation of the imaging agent. Importantly, the major difference between the use of a functional polymer like PGMA as an anchoring and the traditional method of attaching to the surface of a nanoparticle lies in the mobility of the epoxide functional groups located in the loops and tails of the core macromolecule. The mobility of the reactive loops of PGMA ensures greater access to anchoring, resulting in a 2-3 fold greater grafting density when compared to a monolayer of epoxy groups on a nanoparticle surface of similar dimension.[24] Most importantly PGMA nanoformulations have been previously demonstrated to deliver drugs (small molecules, peptides, nucleic acids) and cross the blood brain barrier with minimal toxicity.[24-28] This makes the polymer an ideal choice for the development of UC-polymeric drug delivery vehicles for applications in the central nervous system.

Experimental

Nanoparticle synthesis and characterisation

The Yb/Er-doped $NaGdF_4$ nanocrystals were prepared according to a previously reported method.[16] Briefly, $GdCl_3.6H_2O$ (0.80 mmol), $YbCl_3.6H_2O$ (0.18 mmol) and $ErCl_3.6H_2O$ (0.02 mmol) were mixed with oleic acid (14 mL) and 1-octadecene (16 ml) and heated with stirring to 150°C under nitrogen to form a homogeneous solution. The solution was then cooled to 50°C, methanol (10 ml) containing NaOH (2.5 mmol) and NH_4F (4 mmol) was slowly introduced and the resulting reaction mixture was then kept under stirring at 50°C for 30 min. Subsequently, methanol in the system was removed by heating at 100°C for 10 min under vacuum followed by heating at 300°C for 1 hour. The reaction mixture was then cooled to room temperature and the resultant nanoparticles were precipitated with ethanol, purified by several cycles of washing/centrifugation with ethanol and finally re-dispersed in THF.

PGMA-UC nanoparticles were prepared using a nonspontaneous emulsification route. The organic phase was prepared by dispersing the UC nanoparticles (20 mg) and dissolving PGMA (Mw = 250 000 g mol^{-1}, 75 mg) in a 1:1:2 mixture of $CHCl_3$:THF:MEK (1.5 ml:1.5 ml:3 ml). The organic phase was added dropwise, with rapid stirring, to an aqueous solution of Pluronic F-108 (1.25% w/v, 30 m) and the emulsion was homogenized with a probe-type ultrasonicator at low power for 1 min. The organic solvents were allowed to evaporate overnight under a slow flow of $N_{2(g)}$. Centrifugation at 3000g for 45 min removed large aggregates and excess polymer. The supernatant was decanted into a 50 ml flask containing PEI (M_W 1300 g mol^{-1}, 50% wt solution, 100 mg) and heated to 80°C for 18 h. The nanoparticles were purified by multiple washes with water. The resulting concentrated particle suspension was aliquoted (ca. 10 × 500 μl) and stored at 4°C for quantification by lyophilization, analysis, and subsequent use. Nanospheres were sterilized by UV irradiation prior to cell-culture. Dynamic light scattering (DLS) measurements of size and zeta potential of nanoparticle preparations were performed on a Malvern Zetasizer instrument. Samples prepared for transmission electron microscopy (TEM) analysis were deposited onto carbon-coated grids and imaged at 120kV on a JEOL JEM-2100 and selected area electron diffraction patterns of the UC nanoparticles were obtained using the JEOL 3000F at 300kV. Upconverting nanoparticles were analysed by drying solutions (100 μg μl^{-1}) of nanoparticles onto glass slides and measuring their upconversion spectra using a custom optical setup. Approximately 500 μg of nanoparticles were added to each slide. The 975 nm excitation light from a laser diode was focused onto the nanoparticles using an objective lens with a numerical aperture (NA) of 0.4. The emitted upconversion fluorescence was collected using the same objective lens and directed to a spectrometer via a dichroic beamsplitter (edge wavelength 900 nm) and a band-pass filter for blocking any returning excitation light (transmission range: 315–710 nm). The peak wavelength of the laser diode is 974.5 nm. The excitation power was adjusted by altering the forward bias current supplied to the laser diode (20–100 mA) and the temperature of the laser diode was held at a constant value of 25°C via the integrated thermoelectric cooler. Proton relaxometry measurements were performed on dilute aqueous suspensions of nanoparticles, using a Bruker minispec mq60 relaxometer, with a frequency of 60 MHz and field strength of 1.4 T. A dilution series of nanoparticle solutions in water was measured to assess concentration-dependent relaxation rates of the suspensions. Gd concentrations were determined using ICP-MS following acid digestion.

Cell culture, viability assay and confocal imaging

All tissue culture reagents were purchased from Invitrogen unless otherwise stated. Rat pheochromocytoma (PC12) cells were cultured in poly-(L-lysine)-coated polystyrene flasks in a humidified atmosphere containing 5% CO_2 at 37°C, and maintained in RPMI1640 medium supplemented with horse serum (10% v/v), fetal bovine serum (5% v/v), L-glutamine (2 mM), penicillin-streptomycin (100 U ml^{-1}, 100 μg ml^{-1}), non-essential amino acids (100 μM) and sodium pyruvate (1 mM).

All well plates were coated with a poly-L-lysine solution for one hour, and rinsed thoroughly with PBS before plating. Cells were seeded at densities of 1 × 10^5 cells ml^{-1} in 96 well plates for the 72 hour assay. The following day, the medium was removed and replaced with UV-sterilised medium containing nanospheres at concentrations of 0 μg ml^{-1}, 0.1 μg ml^{-1}, 1 μg ml^{-1}, 10 μg ml^{-1}, 100 μg ml^{-1} and 250 μg ml^{-1}, respectively (5 replicate wells per concentration). The toxicity of the synthesised nanoparticles was assessed using a live-dead fluorescence assay, utilising 1 μM calcein-AM (green, live cells) and 2 μM ethidium homodimer (red, dead cells) dissolved in PBS to stain the cells (Invitrogen). Viability was quantified by counting all viable cells in four fields of view per well. Fields of view were randomly assigned and consistent for all culture wells. An Olympus IX51 inverted fluorescence microscope was used for cell viability assessments. For statistical analyses on

cell counts for all nanoparticle concentrations, one-way analysis of variance (ANOVA) tests and Bonferroni post-hoc test for comparison of means were performed to determine statistically significant concentration-dependent effects of nanoparticles on cellular viability.

Samples for confocal microscopy were prepared by seeding cells onto glass cover slips, and exposing the cells to 250 µg ml^{-1} nanoparticle solutions in full growth media. After 24 hours, cells were fixed with 4% paraformaldehyde, stained with Hoechst 33342 nuclear dye (Invitrogen) and mounted onto glass slides for confocal imaging. Confocal microscopy was performed using an inverted Leica TCS SP2 confocal microscope. The excitation source was a wavelength-tuneable Ti:Sapphire laser which can be operated both in pulsed and in continuous-wave mode (Mai-Tai, Spectra-Physics, tuning range 710–990 nm). For imaging of the Hoechst stain, the laser was operated in pulsed mode at a centre wavelength of 800 nm with the detection window 400–450 nm. For tracking upconversion nanoparticles, the laser was operated in continuous-wave mode at 975 nm with the detection window 515–675 nm. Imaging was performed using a Leica HCX PL APO 40×, 1.25 NA oil immersion objective lens.

Results and discussion

In the present study, 7.4 ± 1.4 nm NaGdF$_4$:Yb,Er nanoparticles (Fig 1A) were initially synthesised using high-temperature replacement reactions among GdCl$_3$, YbCl$_3$, ErCl$_3$, NH$_4$F, and NaOH in the presence of oleic acid (OA). OA acts as both a particle surface capping agent and co-solvent together with 1-octadecene, as previously reported.[16] The nanoparticles were highly crystalline. This is confirmed by both high resolution TEM images showing the distance between adjacent lattice fringes to be about 0.32 nm which can be indexed as the d-spacing value (111) of cubic NaGdF$_4$:Yb,Er (JCPDS 27-0697) and the corresponding selected area electron diffraction (SAED) pattern of the bulk sample (Fig 1B and C).[29] The UC nanoparticles were further encapsulated in a PGMA nanosphere using emulsion precipitation, following which the surface was modified with a cationic polyethyleneimine (PEI) surface coating *via* a ring-opening reaction with the epoxide groups of PGMA and amines of PEI (see experimental section for synthesis methodology). The attachment of cationic polymers to the surface of polymeric nanoparticles has long been established as an integral modification to enhance nanoparticle interaction with cells and in turn cellular uptake.[22, 24, 25]

In the present case, internalisation is crucial to validate the efficacy of the proposed composition to serve as a multimodal probe within cells. PGMA coated UC nanoparticles were characterised by TEM, DLS and Zeta potential (Fig 1D-F). The size of the cationic nanoparticles was 181.9 nm (PDI = 0.08) with a zeta potential of 43.4±0.5 mV (Fig 1E-F).
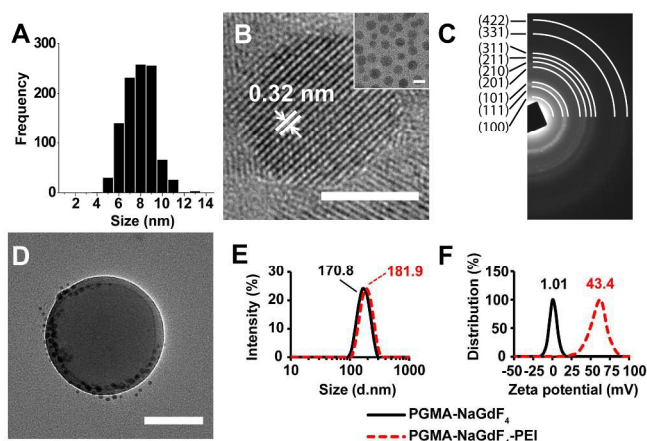

Figure 1. (A) High Resolution TEM image of NaGdF$_4$:Yb,Er nanoparticle at high magnification, scale bar = 5 nm, inset: TEM image of NaGdF$_4$:Yb,Er nanoparticles at low magnification, scale bar = 10 nm. (B) Selected area electron diffraction (SAED) pattern of UC nanoparticles. (C) Size distribution of NaGdF$_4$:Yb,Er nanoparticles. (D) TEM image of a PGMA-NaGdF$_4$:Yb,Er-PEI nanoparticle, scale bar = 100 nm. (E) Hydrodynamic sizes of PGMA-NaGdF$_4$:Yb,Er (170.8 nm; PDI 0.09) and PGMA-NaGdF$_4$:Yb,Er-PEI (181.9 nm; PDI 0.08) nanoparticles as measured by DLS and (F) Zeta potentials of PGMA-NaGdF$_4$:Yb,Er (1.01 ± 0.08 mV) and PGMA-NaGdF$_4$:Yb,Er-PEI (43.4 ± 0.5 mV) nanoparticles.

The polymer nanospheres were then characterised for fluorescence by analysing the UC properties and for MRI contrast by measuring the longitudinal relaxivity (r1) using magnetic resonance relaxometry. Size dependent non-radiative relaxation is often cited as one of the most important limitations in the application of small size UC nanoparticles for cellular imaging, i.e., smaller nanoparticles are associated with weaker emission. This can be overcome by using larger UC nanoparticles. However in the case of multimodality an additional constraint comes into play. In particular, NaGdF$_4$
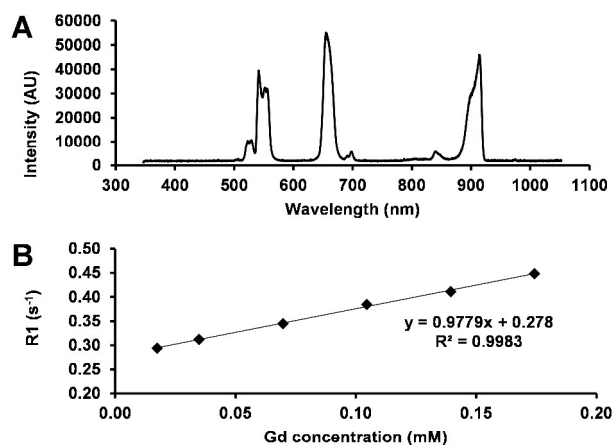

Figure 2. (A) Upconversion fluorescence spectra of PGMA-NaGdF$_4$:Yb,Er-PEI, excited by a 980 nm laser. (B) Longitudinal relaxivity (r1) of PGMA-NaGdF4:Yb,Er-PEI nanoparticles was measured to be 0.98 mM^{-1}s^{-1}.
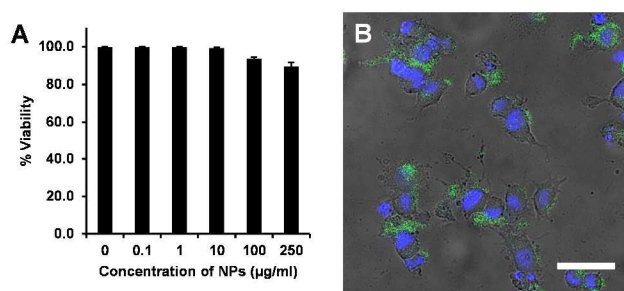
Figure 3. (A) Quantification of viability of PC12 cells incubated with increasing concentrations of PGMA-NaGdF$_4$:Yb,Er-PEI nanoparticles for 72 h, expressed as mean ± SD (one-way ANOVA with Bonferroni post-hoc correction, p > 0.05, N = 5 per group). (B) Confocal images overlaid over a brightfield image of PC12 cells. PGMA-NaGdF$_4$:Yb,Er-PEI nanoparticles (λ_{ex} = 980 nm; λ_{em} = 550/50 nm) are presented as green in the image. Nuclei of PC12 cells are stained with DAPI (blue). Scale bar = 20 μm.

nanoparticles demonstrate a size dependent MRI contrast, with smaller nanoparticles having a greater r1 value. These two opposing size dependent properties have to be balanced for an ideal multimodal imaging agent. In the present case encapsulation of multiple UC nanoparticles within functional core served to maintain both reasonable fluorescence and longitudinal relaxivity.

The fluorescence measurements of the PGMA-UC nanoparticles demonstrated a very strong signal with a Red to Green Emission Ratio (ratio$_{R/G}$) of 1.4. Three major emissions located at 541, 655, and 914 nm were recorded and they are attributed to radiative relaxations from $^2H_{11/2}$, $^4S_{3/2}$, and $^4F_{9/2}$ states to the $^4I_{15/2}$ state of Er^{3+}, respectively, achieved *via* energy transfer processes between Yb^{3+} and Er^{3+} (Fig 2A).

The potential MRI contrast of PGMA coated NaGdF$_4$:Yb,Er nanoparticles was measured by linear regression fitting of the experimental relaxometry data. The molar longitudinal relaxivity, r1, was calculated to be 0.98 mM^{-1}s^{-1} (Fig 2B), which is in agreement with previously reported values.[30]

We next evaluated the biocompatibility of the nanoparticles. It is noteworthy that the nanoparticles were highly stable when stored in physiological conditions over several weeks with no detectable changes. The toxicity of the PEI modified PGMA-UC nanoparticles was examined in PC12 cells after 72 hours incubation. There was no significant decrease in cell viability (*p* > 0.05) for any of the tested concentrations (up to 250 μg ml^{-1}) (Fig. 3A). Following this we assessed the utility of the PGMA-UC nanoparticles as intracellular fluorescent markers using confocal z-stack imaging at λ_{ex} = 980 nm; λ_{em} = 550/50 nm. We observed intense UC fluorescent signals following cellular internalization in PC-12 cells, the representative image shows a single visual slice, thereby demonstrating intracellular location (Fig 3B). It should be noted that while these data indicate internalization of the PGMA-UC nanoparticles quantitative analysis of the number of nanoparticles per cell using either fluorescence or MRI signals upon internalization can prove to be difficult. This is because both these properties are highly sensitive to the local concentration of nanoparticles and the immediate cell-type dependent intracellular environment. For example, the nanoparticle relaxation is known to depend on their compartmentalization in macrophages, lymphocytes, oligodendrocytes, human neural stem cells, and mesenchymal stem cells.[25, 30]

Conclusion

In conclusion, we report a simple methodology using PGMA polymers to develop biocompatible multimodal UC nanoparticles. The use of a reactive PGMA core in combination with UC nanoparticles will enable simple surface modification for site-specific targeting and provide a novel improvement to functionality. Together with the capability for fluorescent and MRI tracking as well as drug delivery, the PGMA-UC nanoparticles may prove useful in clinically relevant models and may lead to the medical translation of UC nanoparticles.

Acknowledgements

References

1 L. Schermelleh, R. Heintzmann and H. Leonhardt, *J. Cell Biol.*, 2010, **190**, 165-175.
2 F. Wang and X. Liu, *Chem. Soc. Rev.*, 2009, **38**, 976-989.
3 F. Wang, D. Banerjee, Y. Liu, X. Chen and X. Liu, *Analyst,* 2010, **135**, 1839-1854.
4 C. Wang, L. Cheng, and Z. Liu, *Biomaterials*, 2011, **32**, 1110-1120.
5 Y. Liu, D. Tu, H. Zhu and X. Chen, *Chem. Soc. Rev.*, 2013, **42**, 6924–6958.
6 M. Haase and H. Schäfer, *Angew. Chem. Int. Ed.*, 2011, **50**, 5808–5829.
7 D. K. Chatterjee, M. K. Gnanasammandhan and Y. Zhang, *Small*, 2010, **6**, 2781–2795.
8 X. Ye, J. E. Collins, Y. Kang, J. Chen, D. T. N. Chen, A. G. Yodh and C. B. Murray, *Proc. Natl. Acad. Sci. U. S. A.*, 2010, **107**, 22430–22435.
9 J. C. Boyer, F. Vetrone, L. Cuccia and J. Capobianco, *J. Am. Chem. Soc.*, 2006, **128**, 7444–7445.
10 F. Wang and X. Liu, *J. Am. Chem. Soc.*, 2008, **130**, 5642–5643.
11 F. Wang, Y. Han, C. S. Lim, Y. Lu, J. Wang, J. Xu, H. Chen, C. Zhang, M. Hong and X. Liu, *Nature*, 2010, **463**, 1061–1065.
12 F. Wang, R. Deng, J. Wang, Q. Wang, Y. Han, H. Zhu, X. Chen and X. Liu, *Nat. Mater.,* 2010, **10**, 968-973.

13   S. Heer, K. Kömpe, H-U. Güdel and M. Haase, *Adv. Mater.*, 2004, **16**, 2102-2105.

14   F. Auzel, *Chem. Rev.*, 2004, **104**, 139–174.

15   A. Xia, M. Chen, Y. Gao, D. Wu, W. Feng and F. Li, *Biomaterials*, 2012, **33**, 5394-5405.

16   C. Liu, Z. Gao, J. Zeng, Y. Hou, F. Fang, Y. Li, R. Qiao, L. Shen, H. Lei, W. Yang and M. Gao, *ACS Nano,* 2013, **7**, 7227–7240.

17   L. Wang, J. Liu, Y. Dai, Q. Yang, Y. Zhang, P. Yang, Z. Cheng, H. Lian, C. Li, Z. Hou, P. Ma and J. Lin, *Langmuir*, 2014, **30**, 13042-13051.

18   T. Paik, T. R. Gordon, A. M. Prantner, H. Yun and C. B. Murray, " *ACS Nano*, 2013, **7**, 2850-2859.

19   G. Tian, W. Yin, J. Jin, X. Zhang, G. Xing, S. Li, Z. Gu and Y. Zhao, *J. Mater. Chem. B*, 2014, **2**, 1379-1389.

20   J. W. Shen, C. X. Yang, L.X. Dong, H.R. Sun, K. Gao and X.P Yan, *Anal. Chem.*, 2013, **85**, 12166-12172.

21   E. Hemmer, F. Vetrone, and K. Soga, *MRS Bull.,* 2014, **39**, 960-964.

22   M. Challenor, P. Gong, D. Lorenser, M. J. House, R. C. Woodward, T. St. Pierre, M. Fitzgerald, S. A. Dunlop, D. D. Sampson and K. Swaminathan Iyer, Dalton Trans., 2014, **43**, 16780-16787.

23   G. A. Silva, *Nat. Rev. Neurosci.*, 2006, **7**, 65-74.

24   C. W. Evans, M. Fitzgerald, T. D. Clemons, M. J. House, B. S. Padman, J. A. Shaw, M. Saunders, A. R. Harvey. B. Zdyrko, I. Luzinov, G. A. Silva, S. A. Dunlop and K. Swaminathan Iyer, *ACS Nano*, 2011, **5**, 8640-8648.

25   C. W. Evans, H. M. Viola, D. Ho, L. C. Hool, S. A. Dunlop, M. Fitzgerald and K. Swaminathan Iyer, *RSC Adv.*, 2012, **2**, 8587-8590.

26   J. Harrison, C. A. Bartlett, G. Cowin, P. K. Nicholls, C. W. Evans, T. D. Clemons, B. Zdyrko, I. A. luzinov, A. R. Harvey, K. Swaminathan Iyer, S. A. Dunlop, M. Fitzgerald, *Small,* 2012, **8**, 1579-1589.

27   I. Lozić, R. V. Hartz, C. A. Bartlett, J. A. Shaw, M. Archer, P. S. R. Naidu, N. M. Smith, S. A. Dunlop, K. Swaminatha Iyer, M. R. Kilburn, M. Fitzgerald, *Biomaterials*, 2016, **74**, 200-216.

28   N. M. Smith, I. Gachulincova, D. Ho, C. Bailey, C. A. Bartlett, M. Norret, J. Murphy, A. Buckley, P. J. Rigby, M. J. House, T. St. Pierre, M. Fitzgerald, K. Swaminathan Iyer, S. A. Dunlop, *Sci. Rep.*, 2016, **6**, 22595; doi: 10.1038/srep22595.

29   J. C. Boyer, J. Gagnon, L. A. Cuccia, J. A. Capobianco, *Chem. Mater.*, 2007, **19**, 3358-3360.

30   N. J. J. Johnson, W. Oakden, G. J. Stanisz, R. S. Prosser, and F. C. J. M. van Veggel, *Chem. Mater.,* 2011, **23**, 3714-3722.

31   C. Billotey, C. Wilhelm, M. Devaud, J. C. Bacri, J. Bittoun, F. Gazeau, *Magn. Reson. Med.* 2003, **49**, 646– 654.

New Journal of Chemistry Accepted Manuscript

TOC:

NaGdF$_4$:Yb,Er nanoparticles with a functional poly(glycidyl methacrylate) (PGMA) coating, as a biocompatible multimodal formulation for neuronal cell imaging.